Original Research Communication

The Association of Peroxiredoxin 4 with the Initiation and Progression of Hepatocellular Carcinoma

Xin Guo[1,2,3], Hirotsugu Noguchi[4], Naoki Ishii[5], Takujiro Homma[5], Taiji Hamada[3], Tsubasa Hiraki[3], Jing Zhang[1], Kei Matsuo[3], Seiya Yokoyama[3], Hiroaki Ishibashi[6], Tomoko Fukushige[7], Takuro Kanekura[7], Junichi Fujii[5], Hidetaka Uramoto[8], Akihide Tanimoto[3], Sohsuke Yamada[1,3]*

Department of [1]Pathology and Laboratory Medicine [6]Oral and Maxillofacial Surgery, and [8]Thoracic Surgery, Kanazawa Medical University, 1-1 Uchinada, Ishikawa, 920-0293, Japan; [2]Laboratory of Pathology, Hebei Cancer Institute, the Fourth Hospital of Hebei Medical University, Jiankang Road 12, Shijiazhuang 050011, Hebei, China; [3]Department of Pathology, and [7]Department of Dermatology, Kagoshima University Graduate School of Medical and Dental Sciences, Kagoshima 890-8544, Japan; [4]Department of Pathology and Cell Biology, School of Medicine, University of Occupational and Environmental Health, 1-1 Iseigaoka, Yahatanishi-ku, Kitakyushu 807-8555, Japan; [5]Department of Biochemistry and Molecular Biology, Graduate School of Medical Science, Yamagata University, 2-2-2 Iidanishi, Yamagata 990-9585, Japan;

Running title: PRDX4 and HCC

***Corresponding author:** Sohsuke Yamada, M.D., Ph.D., Prof., Department of

Pathology and Laboratory Medicine, Kanazawa Medical University, 1-1 Uchinada, Ishikawa, 920-0293, Japan; Tel: 81-76-218-8280; sohsuke@kanazawa-med.ac.jp

Word count (excluding references and figure legends): 5445; **references:** 56; **greyscale illustrations:** 2; **color illustrations: 7; Supplementary illustrations: 10.**

Key words: PRDX4, HCC, oxidative stress, inflammation, cell death

Abstract

Aims: Peroxiredoxin 4 (PRDX4) is a member of the peroxiredoxin family of antioxidant enzymes. Previously, we reported that PRDX4 can restrain the initiation and progression of non-alcoholic steatohepatitis by reducing local and systemic reactive oxygen species (ROS) levels. Oxidative stress is recognized as a key factor in hepatocarcinogenesis, and a high ROS level has also been found in hepatocellular carcinoma (HCC). Here, our aim is to investigate roles of PRDX4 in the initiation and progression of HCC. ***Results:*** In this study, for hepatocarcinogenesis, wild-type (WT), *PRDX4* knockout (*PRDX4*$^{-/y}$) and *human PRDX4* transgenic (*hPRDX4*$^{+/+}$) mice were given a weekly intraperitoneal injection of diethylnitrosamine (DEN) for 25 weeks. The HCC incidence was higher in *PRDX4*$^{-/y}$ mice than in WT or *hPRDX4*$^{+/+}$ mice. Intrahepatic and circulating oxidative stress and inflammatory cell infiltration in the liver were obviously decreased in *hPRDX4*$^{+/+}$ mice, compared to WT mice. Furthermore, in our cohort study, human HCC specimens with low expression of PRDX4 had higher ROS levels and a highly malignant phenotype, which was associated with a reduced overall survival, compared to those with high PRDX4 expression. However, in human HCC cell lines, PRDX4 knockdown led to a rapidly increased intracellular ROS level and suppressed cell proliferation, inducing cell death. ***Innovation and Conclusion:*** Our results clearly indicate that PRDX4 has an inhibitory effect in the initiation of HCC but a dual (inhibitory or promoting) role in the progression of HCC, suggesting the potential utility of PRDX4 activators or inhibitors as therapy for different stages and phenotypes of HCC.

Introduction

Peroxiredoxin 4 (PRDX4), an evolved antioxidant enzyme, is a member of the peroxiredoxin family that includes at least six distinct PRDX genes expressed in mammals (PRDX1-6). In contrast to the solely intracellular localization of other family members, PRDX4 is the only form known to be secreted outside of the cytoplasm, and significant levels have been observed in cultured medium and animal serum. PRDX4 can protect tissues against oxidative damage by scavenging reactive oxygen species (ROS) (mainly toward peroxides) in the intracellular and extracellular space (15, 54). In our previous series studies, elevated levels of PRDX4 were observed in the serum and certain tissues of human and mice with chronic inflammatory diseases, and the over-expression of human PRDX4 (hPRDX4) in mice markedly reduced the local and systemic levels of ROS and suppressed the development and progression of these diseases (14, 17, 32, 34). In particular, we found that PRDX4 can prevent the initiation and progression of non-alcoholic steatohepatitis (NASH) by reducing the expression of oxidative stressors and inflammation, suggesting a beneficial role of PRDX4 in the liver (32, 34).

Hepatocellular carcinoma (HCC) is one of the most common cancers worldwide and the third-most common cause of cancer death, with a rising incidence (52). The initiation of HCC mainly arises from a context of inflammation caused by chronic liver disease (4). Chronic hepatic inflammation will lead to increased oxidative stress. The latter is becoming recognized as a key factor in the progression of chronic liver disease and hepatocarcinogenesis. Recruited inflammatory cells and

activated kupffer cells can produce a large amount of ROS that can conversely affect these cells, causing the further release of chemical mediators, enhancing oxidative stress and increasing the likelihood of hepatocarcinogenesis (30, 53). Thus, the interaction between oxidative stress and persistent inflammatory stimuli plays an important role in the initiation of HCC (11, 43).

Diethylnitrosamine (DEN) is often used as a hepatic carcinogen in the murine model, since DEN-induced HCC has similar histologic and genetic features to human HCC (25). There is evidence that DEN causes the initiation of HCC, depending on the mechanism, with oxidative stress and the inflammation response playing important roles (23, 29). Therefore, a potential role of PRDX4 in the pathogenesis of DEN-induced HCC is of particular interest.

ROS overproduction has been also demonstrated in HCC. Cancer cells have an increased rate of ROS production with an altered redox environment, resulting in higher basal ROS levels in cancer cells than that in their normal counterparts. However, the Warburg effect enables cancer cells to evade excess ROS generated by glucose oxidation from mitochondrial respiration, leading to moderate oxidative stress, which protects cancer cells against ROS-mediated anoikis and allows them to gain a survival advantage over normal cells (28). The higher-than-normal ROS levels that do not damage cancer cells are suggested to be related to tumor growth, angiogenesis and metastasis (16, 27, 41). However, in an environment of increased ROS production, cancer cells still experience a high level of oxidative stress (31). The excess production of ROS caused by various factors produces severe oxidative stress, which

is still toxic to cancer cells and can induce cell death through cell pro-death pathways (5). Thus, the role of PRDX4 in HCC therapy is attracting increasing interest.

In this study, through DEN-induced hepatocarcinogenesis in PRDX4 genovariation mice, immunohistochemistry (IHC) staining of PRDX4 in human HCC tissues, and PRDX4 small interfering RNAs (siRNAs) transfection to human HCC cell lines, we investigated the role of PRDX4 in the initiation and progression of HCC.

Results

Deficiency of PRDX4 enhances hepatocarcinogenesis in mice

There were no significant differences in the appearance or body weight of WT, *PRDX4*$^{-/y}$ and *hPRDX4*$^{+/+}$ mice. The mRNA and protein expression levels of hepatic hPRDX4 and the serum level of hPRDX4 were high in *hPRDX4*$^{+/+}$ mice (Supplementary Fig. 1). To determine the role of PRDX4 in hepatocarcinogenesis, a weekly intraperitoneal injection of DEN (35 mg/kg) or saline (control) was administered to 3- to 4-week-old WT, *PRDX4*$^{-/y}$ and *hPRDX4*$^{+/+}$ male mice, and based on our pilot studies (Supplementary Fig. 2), animals were sacrificed after 25 injections of DEN or saline. None of the mice that received a weekly intraperitoneal injection of saline developed HCC (Supplementary Fig. 3A). A significant increase in the HCC incidence rate was observed in *PRDX4*$^{-/y}$ mice, compared to WT or *hPRDX4*$^{+/+}$ mice, while no marked difference in HCC incidence was found between WT and *hPRDX4*$^{+/+}$ mice (Table 1 and Supplementary Fig. 3A, B). Accordingly, the serum level of alpha-fetoprotein (AFP) was increased in DEN-treated *PRDX4*$^{-/y}$ mice. Chronic liver disease may induce the production of AFP; thus, an increased AFP level was also observed in the serum of WT mice after DEN treatment (Supplementary Fig. 4). To further determine the role of PRDX4 for hepatocarcinogenesis, a long-term observation of 24 months was carried out in WT, *PRDX4*$^{-/y}$ and *hPRDX4*$^{+/+}$ male mice under natural conditions. Consistent with the DEN-induced HCC model, a dramatic increase in tumor incidence was observed in 24-month-old PRDX4$^{-/y}$ mice, while no tumor incidence occurred in age-matched WT and *hPRDX4*$^{+/+}$ mice (Table 1 and

Supplementary Fig. 5).

Multiple tumor nodules were observed in the liver of *PRDX4*$^{-/y}$ mice (Fig. 1A), and histologically, DEN-induced tumors were hepatocyte tumors with the typical features of HCC, including enlarged round hyperchromatic nuclei, high nuclear-cytoplasmic ratios, and moderate micro- or macrovesicular fat globules in the cytoplasm (Fig. 1B). Azan and silver staining showed the carcinoma cells are not surrounded by reticulin fibers, but adjacent liver cells were clearly surrounded by reticulin fibers (Fig. 1C).

Overexpression of PRDX4 protect liver from DEN-induced injury in mice

Although there were no significant differences in the HCC incidence between WT and *hPRDX4*$^{+/+}$ mice, the number of infiltrated neutrophils was less in the liver of *hPRDX4*$^{+/+}$ mice than in WT mice exposed to DEN for 15 or 25 weeks (Fig. 2A). Furthermore, the number of 8-OHdG positive hepatocytes in the liver was significantly lower in *hPRDX4*$^{+/+}$ mice at 15 or 25 weeks after DEN treatment than in WT mice (Fig. 2B), and the level of TBARS (a) and H_2O_2 (b) in the serum was also lower in *hPRDX4*$^{+/+}$ mice than in WT mice at 25 weeks after DEN treatment (Fig. 2C), indicating that the overexpression of hPRDX4 had reduced the local and circulating oxidative stress status in mice treated with DEN. The level of aspartate aminotransferase (AST) and alanine aminotransferase (ALT) in the serum was also lower in *hPRDX4*$^{+/+}$ mice than in WT mice at 25 weeks after DEN treatment (Fig 2D). These results suggest that PRDX4 can protect hepatocytes from DEN-induced injury

that is closely associated with the initiation of HCC.

Low expression of PRDX4 with high ROS levels was correlated with disease progression and a reduced overall survival in human HCC

To evaluate the clinical significance of PRDX4 in human HCC, we investigated the PRDX4 expression by IHC staining of 86 human HCC tissues. Based on the IHC staining scores evaluated by three professional pathologists, cases were divided into two groups—low- and high-PRDX4 groups—using a receiver operating characteristic (ROC) curve (Table 2, Fig. 3A). The clinicopathological characteristics were compared between the two groups (Table 2). The low-PRDX4 group exhibited larger tumor size and more portal and hepatic vein invasion, than the high-PRDX4 group, suggesting that tumors with low PRDX4 expression had more aggressive characteristics than those with high PRDX4 expression. Accordingly, a Kaplan-Meier's survival analysis (Fig. 3B) indicated that the low-PRDX4 group had a significantly reduced overall survival compared to the high-PRDX4 group. Fruthermore, using IHC staining, we evaluated the expression of 8-hydroxy-2'-deoxyguanosine (8-OHdG) as a marker for oxidative stress to determine the status of oxidative stress in tumor tissues (Fig. 3C) and found that the 8-OHdG level was higher in the low-PRDX4 group than in the high-PRDX4 group (Fig. 3D). Thus, PRDX4 may suppress tumor growth and invasion by downregulating the intracellular ROS level of cancer cells, which is associated with the disease prognosis.

Down-regulation of PRDX4 enhances the ROS level but represses cell proliferation in HCC cell lines

To further determine the role of PRDX4 in HCC cells, we knocked down its expression in PLC/PRF/5 and HepG2 cells using three kinds of PRDX4-specific siRNAs. Real-time polymerase chain reaction (PCR) showed that siRNAs (HSS116214) were the most efficient at knock-down of PRDX4 (Fig. 4A). A significant reduction in the PRDX4 mRNA and protein expression was observed at days 1 and 3, respectively, after transfection with PRDX4 siRNAs (HSS116214) (Fig. 4B). Viability assays using the Cell Counting Kit-8 showed that the proliferation of PLC/PRF/5 and HepG2 cells was significantly suppressed after PRDX4 expression was down-regulated (Fig. 4C). Fluorescence microscopy revealed that the number of dihydroethidium (DHE)-positive (Fig. 4D) and DCF-positive (Fig. 4E) cells was much greater among HCC cells transfected with PRDX4 siRNAs than among those cells transfected with negative siRNAs. These results support the notion that PRDX4 has very important roles in redox homeostasis of HCC cells, which may affect cancer cell proliferation.

PRDX4 knockdown affects the HCC cell survival

A flow cytometry assay showed no significant difference in the number of apoptotic cells three days after transfection with PRDX4 or negative siRNAs. However, the ratio of sub-G1 was higher at 5 and 7 days after transfection with PRDX4 siRNAs than after that with negative siRNAs (Fig. 5A). In addition, the number of

TUNEL-positive cells was significantly greater among HCC cells transfected with PRDX4 siRNAs than among those transfected with negative siRNAs (Fig. 5B). In line with the increased apoptosis, a large number of PRDX4-knockdown cells were found in the medium at 7 days after transfection, while cells with normal PRDX4 expression remained firmly attached to the culture dish (Fig. 5C). Supporting these observations, Western blotting showed that the protein expression of cleaved caspase-3 was significantly higher in PRDX4 siRNAs-transfected HCC cells than in negative siRNA-transfected HCC cells (Fig. 5D).

The intracellular ROS level is also closely associated with another cell pro-death pathway: autophagy. A significant increase in the number of CYTO-ID-positive cells was observed in those cells transfected with PRDX4 siRNAs compared to negative siRNAs (Fig. 6A, B). An ultrastructural analysis also showed that a large number of autophagosomes and/or autolysosomes were observed in PRDX4-knockdown HCC cells (Fig. 6C and Supplementary Fig. 6). The analysis of protein expression of some autophagy-related genes showed that the expression of microtubule-associated protein light chain (LC) 3-II was increased while that of autophagy-related gene (Atg) 4 was decreased at 5 days after HCC cells were transfected with PRDX4 siRNAs (Fig. 6D). These data indicate that increased oxidative stress caused by down-regulating PRDX4 expression triggered cell death pathways through not only apoptosis but also autophagy.

Discussion

In this study, our results showed that the deficiency of PRDX4 promoted DEN-induced hepatocarcinogenesis in mice, low PRDX4 expression enhanced tumor growth and invasion with a reduced overall survival in human HCC, but down-regulation of PRDX4 suppressed cell proliferation and induced cell death in human HCC cell lines. We suggest that PRDX4 may play important roles in the initiation and progression of HCC.

All the time, it is widely accepted that PRDXs act as tumor 'preventers' (35). Indeed, loss of PRDXs could promote carcinogenesis in mice. For example, *PRDX1*-knockout mice exhibit a shortened lifespan owing to be predisposed to the development of haemolytic anaemia and several malignant cancers (36). Deficiency of PRDX6 in mice enhanced the susceptibility to 7,12-dimethylbenz[a]anthracene (DMBA)/ 12-O-tetradecanoylphorbol 13-acetate (TPA)- or human papilloma virus 8 (HPV8)–induced skin tumorigenesis (44). Similar to these data, in the present study, a markedly higher HCC incidence was observed in *PRDX4*$^{-/y}$ mice 25 weeks after i.p. DEN weekly, compared to WT or *hPRDX4*$^{+/+}$ mice. Whereas, overexpression of PRDX4 reduced intrahepatic and circulating ROS level and suppressed leukocyte infiltration in the liver of mice exposed to DEN. A large amount of ROS generated by the P450-dependent enzymatic system during the process of DEN biotransformation can affect hepatocyte replication, proliferation and apoptosis through multiple signal pathways (3, 38, 46), leading to hepatocarcinogenesis. In addition, oxidative stress can accelerate the infiltration and activation of inflammatory cells and the excessive

release of inflammatory factors, which can enhance DEN-induced hepatocarcinogenesis (33). Our previous results have indicated that PRDX4 can prevent endothelial dysfunction and decrease expression of adhesion molecules and inflammatory cell migration (14, 17, 32, 34). Therefore, combining these results suggests that PRDX4 may have an efficient effect in inhibiting ROS/inflammation-related hepatocarcinogenesis.

A large amount of clinical evidences have indicated that PRDXs also play important roles in malignant progression of many cancers and have potential clinical implications in cancer therapy, where PRDXs function as a tumor suppressor or promoter (7, 13, 37, 42, 47-48). The overexpression of PRDX4 was identified in oral and prostate cancer tissues and was found to be associated with a positive pN status and tumor cell proliferation (9, 51), while the expression of the antioxidant protein is downregulated in acute promyelocytic leukemia (39). Interestingly, a report showed that the high expression of PRDX4 in tumor tissues was significantly correlated with higher recurrence rates and shorter disease-free survival (DFS) in patients with lung squamous cell carcinoma, but not in patients with lung adenocarcinoma (18). Our clinicopathological analysis displayed that low PRDX4 expression promoted tumor growth and invasion with a higher ROS level, which is closely related to a reduced overall survival, implying PRDX4 may be a tumor suppressor in HCC. Whereas, our *in vitro* data showed that down-regulation of PRDX4 expression inhibited cell proliferation and induced death in HCC cell lines, suggesting PRDX4 may also be a promoter of HCC. These results may seem contradictory, but they should be plausible

because of the ‘‘two-faced’’ property of ROS. A great number of studies confirm that moderate oxidative stress can lead to cancer progression, whereas severe oxidative stress will cause cancer cell death (1, 10). In current *in vitro* experiments, a sudden decrease of PRDX4 expression led to a mass rapid accumulation of intracellular ROS, which probably cause severe oxidative stress, directly resulting in cell growth inhibition and death. However, in human HCC tumors with low PRDX4 expression, a possible explanation is that an adaptable redox homeostasis may exist and enable cancer cells to tolerate a higher level of ROS that contribute for malignant progression (49), suggesting PRDX4 may have a key role in the process of new redox homeostasis formation caused by high metabolism of cancer cells. Our current understanding of the function of PRDX4 is still lacking in cancer, and further research must be undertaken to better understand these findings.

Inducing cancer cell apoptosis is a widely acceptable strategy for cancer therapy (6), since cancer cells may be more sensitive to the toxic generated by the accumulation of excess ROS by inducing big amounts of ROS or damaging the ROS scavenging capacity of cells, which potentially induce cell death. Indeed, our results showed that down-regulation of PRDX4 expression enhanced intracellular ROS level and induced cell apoptosis in HCC cell lines, which is also supported by other research (21). Interestingly, in this study, besides apoptosis, we also found PRDX4 is also closely associated with another cell pro-death pathway, autophagy (12). Many anti-cancer treatments have been shown to activate autophagy, and therapeutic induction of autophagy-related cell death is obtaining widespread attention in cancer

therapy strategies (8, 55). Our *in vitro* results confirm that enhanced ROS level caused by PRDX4 knockdown led to the inactivation of Atg4, which promoted lipidation of Atg8 (LC3), a key step during autophagosome formation (45), thereby increasing autophagy activity in HCC cells. Similar results were also observed in breast cancer cells treated with carnosol that induced ROS-related autophagy and apoptosis leading to cell death (2). However, the consideration is probably oversimplified, as the complexity of cellular effects have been observed in various anti-cancer treatments, where ROS-induced autophagy cause either cell death or drug resistance or both, showing autophagy can also protect against cellular stress (40). In addition, emerging evidence suggests the multiple layers of crosstalk between autophagy and apoptosis, depending on interactions among the crucial proteins involved in them (24, 56). At present, we cannot delineate that an increase in autophagy accelerated cell death or was only a protect response to oxidative stress. Further studies are necessary to confirm the role of autophagy and its relationship with apoptosis in HCC.

There are still some research limitations in the present study. (i) Although we suggested an inhibitory effect of PRDX4 in hepatocarcinogenesis, DEN treatment employed in this study did not produce a significant difference in HCC incident between WT and *hPRDX4*$^{+/+}$ mice. A lower dose, longer induction of DEN may be needed to identify the difference in hepatocarcinogenesis between these mice. (ii) Our IHC results showed obvious differences in the expression levels of PRDX4 between adjacent noncancerous liver tissues. Thus, it may be interesting to analyze PRDX4 expression in a larger number of normal liver and HCC samples and to monitor these

patients with regard to HCC initiation and progression. (iii) PLC/PRF/5 and hepG2 cells were also transfected with PRDX4-plasmid DNAs to up-regulate its expression, but over-expression of PRDX4 did not affect these cells survival, probably due to these cells originally having a high PRDX4 level. As far as we know, high PRDX4 expression is observed in almost all of the HCC cell lines (Gene Expression Omnibus database), and thus, primary culture from HCC tumors with low PRDX4 expression may be a good way to identify the effect of additional PRDX4 in HCC progression and clinical outcome.

In summary, our present data indicate that PRDX4 can restrain DEN-induced hepatocarcinogenesis in mice by reducing intrahepatic and circulating oxidative stress, as well as the inflammation response in the liver. However, due to the contradictory property of ROS, PRDX4 plays a dual role in the progression of HCC, promoting the survival of cancer cells but inhibiting the rapid growth and invasion of tumor. We summarized the roles of PRDX4 in HCC in Fig 7. These results may provide a novel treatment strategy for HCC and highlight the importance of antioxidant enzymes in the pathogenesis of cancer.

Innovation

Targeting antioxidants for cancer therapy remains a very controversial issue. The relationship between PRDXs and cancer has garnered widespread attention for its specific antioxidant properties. However, the role of PRDX4 has rarely been investigated in cancer. Here, we investigated the role of PRDX4 in HCC, suggesting that PRDX4 has an inhibitory effect in the initiation of HCC but a dual (inhibitory or promoting) role in the progression of HCC and highlight the importance of antioxidant enzymes in the pathogenesis of cancer. These findings provide novel insights into the role of PRDX4 in cancer and evidence to support the application of antioxidase activators or inhibitors in cancer therapy.

Materials and Methods

Animals and treatment

PRDX4 knockout (*PRDX4*$^{-/y}$) and *hPRDX4* transgenic (*hPRDX4*$^{+/+}$) mice were generated and genotyped as previously described (10, 12, 14, 27, 29). Briefly, for the generation of *PRDX4*$^{-/y}$ mice, PRDX4 genomic DNA was cloned from a b129/SVJ mouse genomic library (Stratagene, CA, U.S.A.). Blastocysts containing ES (embryonic stem) cells in which homologous recombination had occurred were implanted into the uteri of pseudopregnant C57BL/6 female mice. For the construction of *hPRDX4*$^{+/+}$ mice, based on a published sequence (Genebank accession no.NM_006406), hPRDX4 cDNA was amplified and cloned into the pGEM-T easy vector system (Invitrogen, Life Technologies Japan Ltd., Tokyo, Japan). The entire nucleic acid sequence was microinjected into the male pronuclei of one-cell C57BL/6 female mouse embryos. C57BL/6 inbred mice were used as control animals. These mice were maintained in a temperature- and light-controlled facility under a standard 12 h light-dark cycle, fed standard rodent chow, and given water *ad libitum*. For hepatocarcinogenesis, experiments were performed using 3- to 4-week-old male wild-type (WT), *PRDX4*$^{-/y}$ and *hPRDX4*$^{+/+}$ mice weighing 10-14 g who were given a weekly intraperitoneal injection (i.p.) of DEN (35 mg/kg) or saline (negative control) for 25 weeks. In addition, the HCC spontaneous rate was observed in these mice under natural conditions for 24 months.

All protocols were approved by the Ethics Committee of Animal Care and Experimentation, Kagoshima University, Japan, and were performed according to the

Institutional Guidelines for Animal Experiments and the Law (no. 105) and Notification (no. 6) of the Japanese Government. The study also conforms to the Guide for the Care and Use of Laboratory Animals published by the US National Institutes of Health (NIH Publication No. 85-23, revised 1996).

Patients and HCC specimens

Eighty-six clinical tissue samples of HCC with clinicopathological information were collected from HCC patients who underwent hepatic resection at Kagoshima University Hospital between 2008 and 2012 in this study. All formalin-fixed, paraffin-embedded specimens were used for the IHC study (22). A five-year follow-up was conducted after operation. The Ethics Committee of Kagoshima University approved the experimental and research protocols.

Cell culture

The human HCC cell lines PLC/PRF/5 and HepG2 were purchased from Japanese Collection of Research Bioresources Cell Bank (JCRB, Osaka, Japan). These cells were cultured in Dulbecco's Modified Eagle Medium (DMEM) with 10% fetal calf serum and maintained in a humidified atmosphere at 37°C and 95% air/5% CO_2.

siRNA transfection

Three kinds of siRNAs specific for PRDX4 (Stealth siRNAs HSS116212, HSS116214 and HSS173720) were purchased from Invitrogen (Carlsbad, CA, USA). The cells

were plated in 6-well plates and cultured in the growth media at approximately 60% confluence, incubated for 24 h, and transfected for 72 h with 20 nM siRNA duplexes in Lipofectamine® RNAiMAX and Opti-MEM medium (Life Technologies, Carlsbad, CA, USA). Stealth RNAi™ siRNA Negative Control was used as a negative control (Stealth RNAi™, Life Technologies).

Histology and IHC

For histocytological analyses of human HCC specimens and mouse liver, images of staining with hematoxylin and eosin (H&E), silver or azan, or IHC sections were captured and quantified using the NanoZoomer Digital Pathology Virtual Slide Viewer software program (Hamamatsu Photonics Corp., Hamamatsu, Japan) (20). To detect hPRDX4 expression in human HCC tissues, we used a rabbit anti-human polyclonal antibody (1:100; Affinity BioReagents, Golden, CO, USA) incubated at 4° C during overnight, and a goat polyalkaline phosphatase secondary antibody (Vulcan Fast Red; Biocare Medical, Concord, CA, USA). To analyze the ROS/oxidative stress levels in cancer cells of mouse liver or human HCC tumor tissues, we used an anti-8-OHdG monoclonal antibody (1:200; Japan Institute for the Control of Aging, Fukuroi, Japan), and staining scores were evaluated by three professional pathologists. The endogenous peroxidase activity was not blocked for the analysis of oxidative stress markers. Silver staining and azan staining were used for the observation of reticulin fibers around the tumor cells in *PRDX4*$^{-/y}$ mice.

Blood sample measurements

Thiobarbituric acid reactive substances (TBARS) are a well-established method for evaluating lipid peroxidation, and were used as an index of lipid peroxidation and oxidative stress. To assess a second and more quantitative marker of oxidative stress, we measured the TBARS levels using a TBARS Assay Kit (Cayman Chemical Company, Ann Arbor, MI, USA) in serum collected from DEN- or saline-injection mice. Results are expressed as -μM MDA. The serum levels of hPRDX4 (hPRDX4 ELISA Kit; Abnova, Taipei, Taiwan) and AFP (Mouse AFP ELISA kit; Cloud-Clone Corp. Houston USA) in DEN-treated mice were measured using ELISA kits according to the manufacturers' instructions. The serum levels of ALT and AST were measured using an automatic blood analyzer JCA-BM6070 (BioMajesty™, Japan). For the assessment of the hydroperoxide levels, a diacron reactive oxygen metabolites (dROM) test was performed using a an FRAS4 System (H&D, Parma, Italy), as described previously (50). The units of this measurement are expressed as Ucarr (Carratelli unit) values, where one unit corresponds to 0.8 mg/L hydrogen peroxide.

Real-Time RT-PCR

Total RNA from HCC cells was extracted using Total RNA Extraction Miniprep System (Viogene BioTek, New Taipei City, Taiwan) and stored at -80°C until analysis. Total RNA was converted into cDNA using a High Capacity RNA-to-cDNA Kit (Life Technologies). The cDNA was analyzed by a LightCycler® 96 (Roche Diagnostics, Tokyo, Japan) and subjected to 40 cycles of amplification using TaqMan gene

expression assays (Life Technologies). Each sample was analyzed in triplicate in separate wells for PRDX4 and ribosomal *18S* genes. The average of three threshold cycle values for the target and *18S* genes were calculated, and then analyzed using the comparative Ct method. Custom made primers and TaqMan probe for PRDX4 gene amplification were purchased from Life Technologies (Assay ID: Hs01056076_m1).

Western blotting

Proteins (20 mg) isolated from HCC cells were separated by SDS-PAGE and transferred to Immun-Blot polyvinylidene difluoride membranes (Bio-Rad Laboratories, K.K., Tokyo, Japan) using a semidry blotter (26). After transfer onto polyvinylidene difluoride membranes, the membranes were blocked with 5% non-fat milk in TBST (20 mmol/L Tris-HCl (pH 7.6), 150 mmol/L sodium chloride, and 0.1% Tween 20) for 1 h at room temperature (RT) and then incubated overnight at 4°C with primary antibody diluted in Can Get Signal solution 1 (Toyobo, Osaka, Japan) and with a horseradish peroxidase conjugated goat anti-rabbit antibody (MP Biomedicals, Santa Ana, CA) for 1 h at RT. The following primary antibodies and dilutions were used: rabbit polyclonal antibody to hPRDX4 (1:1000; Santa Cruz Biotechnology), rabbit monoclonal antibodies to Atg4 (D62C10), LC3 (D3U4C), caspase-3 (8G10), cleaved caspase-3 (5A1E), and β-actin (13E5) (Cell Signaling Technology, Danvers, MA) (Supplementary Fig. 7-10). Protein expression was detected with SuperSignal West Pico chemiluminescent substrate or SuperSignal West Femto Maximum Sensitivity Substrate (Thermo Scientific). Densitometry analysis was performed with

NIH ImageJ software version 1.43.

Cell proliferation assay

The viability of cells was measured using the CCK-8 method according to the manufacturer's instructions. After transfection with siRNAs, 3×10^3 PLC/PRF/5 or HepG2 cells were seeded in one well of 96-well plates respectively, allowed to attach for 16 h, and observed for viability for 72 h. The absorbance at 450 nm was measured using a microplate reader. Six replicate wells were used for each group.

Detection of intracellular ROS

The intracellular ROS level was assessed with two oxidation-sensitive fluorescent dyes, DHE (Molecular Probes, Eugene, OR, USA) and CM-H2DCF-DA (Molecular Probes) for HCC cell lines. PLC/PRF/5 cells were transfected with PRDX4 or negative siRNA for 72 h, and then cells were rinsed quickly with Krebs–Ringer solution and incubated with freshly prepared 5 μM DHE or CM-H2DCF-DA for 5 min, respectively. After staining, we quantified the number of positive-cells (those with increased DHE- or DCF- associated fluorescence in 10 randomly selected fields per section; original magnification: × 400), as described previously.

Flow cytometric analysis of cell cycle and apoptosis

The HCC cells were transfected with PRDX4 or negative siRNA for 3 days, 5 days and 7 days then collected and washed twice with cold phosphate buffered saline

(PBS). Cells were fixed in 70% ethanol at -20 °C, and then washed with phosphate-buffered saline. The cells were then incubated with phosphate-citrate buffer (pH 7.8) at RT for 30 min and resuspended in 1 mL of propidium iodide solution (50 μg/mL) containing 50 μL of RNase A solution (10 mg/mL). After suspensions were incubated for 30 min on ice, DNA content was analyzed using a CyAn-ADP flow cytometer (Beckman Coulter, Brea, CA).

Detection of autophagy

The autophagic vacuoles in HCC cells transfected with siRNAs were determined using a Cyto-ID autophagy detection kit 2.0 (Enzo Life Sciences, Farmingdale, NY, USA) according to the manufacturer's instructions.

TUNEL staining

To determine the number of apoptotic cells in PRDX4 or negative siRNA-transfected PLC/PRF/5 cells, we conducted TUNEL assays using the *in situ* Cell Death Detection Kit, POD (Roche Applied Science, Lewes, United Kingdom). After staining, the number of positive-cells was quantified as described above.

Ultrastructural analysis

PLC/PRF/5 cells transfected with PRDX4 or negative siRNAs were fixed with 2.5% glutaraldehyde in 0.1 M Na Cacodylate, pH 7.4 for 2 h, postfixed with 2% aqueous osmium tetroxide for 2.5 hours, and subsequently stained en bloc in 2.5% uranyl

acetate (in water) overnight before dehydration and embedding in Eponate 12 resin (Ted Pella, Inc., Redding, CA, USA). Thick (1 μm) sections of the embedded cells were examined at the light microscopic level. The cell blocks were further trimmed to obtain thin sections (80 nm), stained with saturated solution of uranyl acetate (15 min) followed by Reynolds' lead citrate (8 min), and view on a transmission electron microscopyed on a transmission electron microscopy (JEM-1200EX; JEOL Ltd., Tokyo, Japan).

Statistical analysis

All statistical analyses were performed with EZR (Saitama Medical Center, Jichi Medical University, Saitama, Japan), the graphical user interface for R (The R Foundation for Statistical Computing, version 2.13.0, Vienna, Austria). Categorical variables were compared using χ^2 tests or Fisher's exact tests. A Kaplan-Meier's analysis was used to analyze the overall survival, and survival curves were compared using log-rank tests. Statistical analyses were performed for continuous variables using Student's or Welch's *t*-test. All statistical tests were 2-sided, and differences and correlations values of $P < 0.05$ were considered statistically significant.

Acknowledgments

We would like to thank Orie Iwaya, Mai Tokudome, and Yoshie Jidouhou for their expert technical assistance; we thank the patients for taking part in this study. This study was supported by grants from National Natural Science Foundation of China

(No. 81402490) (to X.G.), Natural Science Foundation of Hebei Province (No. H2016206170) (to X.G.), High level talent support project of Hebei Province (No. CG2015003011) (to X.G.), the Kodama Memorial Fund for Medical Research, Kagoshima, Japan (to S.Y. and A.T.), and by Grants-in-Aid for Scientific Research (16K08750) from the Ministry of Education, Culture, Sports, Science and Technology, Tokyo, Japan (to S.Y.).

Author Disclosure Statement

No potential conflicts of interest exist.

List of Abbreviations

8-OHdG = 8-hydroxy-2'-deoxyguanosine

AFP = alpha-fetoprotein

ALT = alanine aminotransferase

AST = aspartate aminotransferase

Atg = autophagy-related gene

dROM = diacron reactive oxygen metabolites

DEN = diethylnitrosamine

DHE = dihydroethidium

DMEM = Dulbecco's Modified Eagle Medium

DMBA = 7,12-dimethylbenz[a]anthracene

H&E = hematoxylin and eosin

HCC = hepatocellular carcinoma

hPRDX4 = human peroxiredoxin 4

HPV8 = human papilloma virus 8

IHC = immunohistochemistry

i.p. = intraperitoneal injection

LC = microtubule-associated protein light chain

MDA = malondialdehyde

NASH = non-alcoholic steatohepatitis

PBS = phosphate buffered saline

PRDX4 = Peroxiredoxin 4

ROC = receiver operating characteristic

ROS = reactive oxygen species

RT = room temperature

siRNAs = small interfering RNAs

TBARS = thiobarbituric acid reactive substances

TPA = 12-O-tetradecanoylphorbol 13-acetate

TUNEL = terminal deoxynucleotidyl transferase end-labeling

WT = wild type

References

1. Afanas'ev I. Reactive oxygen species signaling in cancer: comparison with aging. *Aging Dis* 2: 219–230, 2011.

2. Al Dhaheri Y, Attoub S, Ramadan G, Arafat K, Bajbouj K, Karuvantevida N, AbuQamar S, Eid A, Iratni R. Carnosol induces ROS-mediated beclin1-independent autophagy and apoptosis in triple negative breast cancer. *PLoS ONE* 9: e109630, 2014.

3. Amstad P, Crawford D, Muehlematter D, Zbinden I, Larsson R, Cerutti P. Oxidants stress induces the proto-oncogenes c-fos and cinogenesis c-myc in mouse epidermal cells. *Bull Cancer* 77: 501–502, 1990.

4. Aravalli RN, Steer CJ, Cressman EN. Molecular mechanisms of hepatocellular carcinoma. *Hepatology* 48: 2047–2063, 2008.

5. Benhar M, Dalyot I, Engelberg D, Levitzki A. Enhanced ROS production in oncogenically transformed cells potentiates c-Jun N-terminal kinase and p38 mitogen-activated protein kinase activation and sensitization to genotoxic stress. *Mol Cell Biol* 21: 6913–6926, 2001.

6. Bremer E, van Dam G, Kroesen BJ, de Leij L, Helfrich W. Targeted induction of apoptosis for cancer therapy: current progress and prospects. *Trends Mol Med* 12: 382–393, 2006.

7. Byun JM, Kim SS, Kim KT, Kang MS, Jeong DH, Lee DS, Jung EJ, Kim YN, Han J, Song IS, Lee KB, Sung MS. Overexpression of peroxiredoxin-3 and -5 is a potential biomarker for prognosis in endometrial cancer. *Oncol Lett* 15: 5111–5118,

2018.

8. Carew JS, Kelly KR, Nawrocki ST. Autophagy as a target for cancer therapy: new developments. *Cancer Manag Res* 4: 357–365, 2012.

9. Chang KP1, Yu JS, Chien KY, Lee CW, Liang Y, Liao CT, Yen TC, Lee LY, Huang LL, Liu SC, Chang YS, Chi LM. Identification of PRDX4 and P4HA2 as metastasis-associated proteins in oral cavity squamous cell carcinoma by comparative tissue proteomics of microdissected specimens using iTRAQ technology. *J Proteome Res* 10: 4935–4947, 2011.

10. Chio IIC, Tuveson DA. ROS in Cancer: The Burning Question. *Trends Mol Med* 23: 411–429, 2017.

11. Del Campo JA, Gallego P, Grande L. Role of inflammatory response in liver diseases: Therapeutic strategies. *World J Hepatol* 27;10: 1–7, 2018.

12. Denton D, Xu T, Kumar S. Autophagy as a pro-death pathway. *Immunol Cell Biol* 93: 35–42, 2015.

13. Ding C, Fan X, Wu G. Peroxiredoxin 1 - an antioxidant enzyme in cancer. *J Cell Mol Med* 21: 193–202, 2017.

14. Ding Y, Yamada S, Wang KY, Shimajiri S, Guo X, Tanimoto A, Murata Y, Kitajima S, Watanabe T, Izumi H, Kohno K, Sasaguri Y. Overexpression of peroxiredoxin 4 protects against high-dose streptozotocin-induced diabetes by suppressing oxidative stress and cytokines in transgenic mice. *Antioxid Redox Signal* 13: 1477–1490, 2010.

15. Fujii J, Ikeda Y, Kurahashi T, Homma T. Physiological and pathological views of

peroxiredoxin 4. *Free Radic Biol Med* 83: 373–379, 2015.

16. Gill JG, Piskounova E, Morrison SJ. Cancer, Oxidative Stress, and Metastasis. *Cold Spring Harb Symp Quant Biol* 81: 163–175, 2016.

17. Guo X, Yamada S, Tanimoto A, Ding Y, Wang KY, Shimajiri S, Murata Y, Kimura S, Tasaki T, Nabeshima A, Watanabe T, Kohno K, Sasaguri Y. Overexpression of peroxiredoxin 4 attenuates atherosclerosis in apolipoprotein E knockout mice. *Antioxid Redox Signal* 17: 1362–1375, 2012.

18. Hwang JA, Song JS, Yu DY, Kim HR, Park HJ, Park YS, Kim WS, Choi CM. Peroxiredoxin 4 as an independent prognostic marker for survival in patients with early-stage lung squamous cell carcinoma. *Int J Clin Exp Pathol* 8: 6627–6635, 2015.

19. Iuchi Y, Okada F, Tsunoda S, Kibe N, Shirasawa N, Ikawa M, Okabe M, Ikeda Y, Fujii J. Peroxiredoxin 4 knockout results in elevated spermatogenic cell death via oxidative stress. *Biochem J* 419: 149–158, 2009.

20. Kawatsu Y, Kitada S, Uramoto H, Zhi L, Takeda T, Kimura T, Horie S, Tanaka F, Sasaguri Y, Izumi H, Kohno K, Yamada S. The combination of strong expression of ZNF143 and high MIB-1 labelling index independently predicts shorter disease-specific survival in lung adenocarcinoma. *Br J Cancer* 110: 2583–2592, 2014.

21. Kim TH, Song J, Alcantara Llaguno SR, Murnan E, Liyanarachchi S, Palanichamy K, Yi JY, Viapiano MS, Nakano I, Yoon SO, Wu H, Parada LF, Kwon CH. Suppression of peroxiredoxin 4 in glioblastoma cells increases

apoptosis and reduces tumor growth. *PLoS ONE* 7: e42818, 2012.

22. Kitada S, Yamada S, Kuma A, Ouchi S, Tasaki T, Nabeshima A, Noguchi H, Wang KY, Shimajiri S, Nakano R, Izumi H, Kohno K, Matsumoto T, Sasaguri Y. Polypeptide N-acetylgalactosaminyl transferase 3 independently predicts high-grade tumours and poor prognosis in patients with renal cell carcinomas. *Br J Cancer* 109: 472–481, 2013.

23. Kolaja KL, Klaunig JE. Vitamin E modulation of hepatic focal lesion growth in mice. *Toxicol Appl Pharmacol* 143: 380–387, 1997.

24. Lalaoui N, Lindqvist LM, Sandow JJ, Ekert PG. The molecular relationships between apoptosis, autophagy and necroptosis. *Semin Cell Dev Biol* 39: 63–69, 2015.

25. Lee JS, Chu IS, Mikaelyan A, Calvisi DF, Heo J, Reddy JK, Thorgeirsson SS. Application of comparative functional genomics to identify best-fit mouse models to study human cancer. *Nat Genet* 36: 1306–1311, 2004.

26. Li Z, Yamada S, Inenaga S, Imamura T, Wu Y, Wang KY, Shimajiri S, Nakano R, Izumi H, Kohno K, Sasaguri Y. Polypeptide N-acetylgalactosaminyltransferase 6 expression in pancreatic cancer is an independent prognostic factor indicating better overall survival. *Br J Cancer* 104: 1882–1889, 2011.

27. Liou GY, Storz P. Reactive oxygen species in cancer. *Free Radic Res* 44: 479–496, 2010.

28. Lu J, Tan M, Cai Q. The Warburg effect in tumor progression: mitochondrial oxidative metabolism as an anti-metastasis mechanism. *Cancer Lett* 356: 156–164,

2015.

29. Maeda S, Kamata H, Luo JL, Leffert H, Karin M. IKKbeta couples hepatocyte death to cytokine-driven compensatory proliferation that promotes chemical hepatocarcinogenesis. *Cell* 121: 977–990, 2005.

30. Marx J. Cancer research. Inflammation and cancer: the link grows stronger. *Science* 306: 966–968, 2004.

31. Matés JM, Segura JA, Alonso FJ, Márquez J. Oxidative stress in apoptosis and cancer: an update. *Arch Toxicol* 86: 1649–1665, 2012.

32. Nabeshima A, Yamada S, Guo X, Tanimoto A, Wang KY, Shimajiri S, Kimura S, Tasaki T, Noguchi H, Kitada S, Watanabe T, Fujii J, Kohno K, Sasaguri Y. Peroxiredoxin 4 protects against nonalcoholic steatohepatitis and type 2 diabetes in a nongenetic mouse model. *Antioxid Redox Signal* 19: 1983–1998, 2013.

33. Naugler WE, Sakurai T, Kim S, Maeda S, Kim K, Elsharkawy AM, Karin M. Gender disparity in liver cancer due to sex differences inMyD88-dependent IL-6 production. *Science* 317: 121–124, 2007.

34. Nawata A, Noguchi H, Mazaki Y, Kurahashi T, Izumi H, Wang KY, Guo X, Uramoto H, Kohno K, Taniguchi H, Tanaka Y, Fujii J, Sasaguri Y, Tanimoto A, Nakayama T, Yamada S. Overexpression of Peroxiredoxin 4 Affects Intestinal Function in a Dietary Mouse Model of Nonalcoholic Fatty Liver Disease. *PLoS ONE* 11: e0152549, 2016.

35. Neumann CA, Fang Q. Are peroxiredoxins tumor suppressors? *Curr Opin Pharmacol* 7: 375–380, 2007.

36.Neumann CA, Krause DS, Carman CV, Das S, Dubey DP, Abraham JL, Bronson RT, Fujiwara Y, Orkin SH, Van Etten RA. Essential role for the peroxiredoxin Prdx1 in erythrocyte antioxidant defence and tumour suppression. *Nature* 424: 561–565, 2003.

37. Nicolussi A, D'Inzeo S, Capalbo C, Giannini G, Coppa A. The role of peroxiredoxins in cancer. Mol Clin Oncol 6: 139–153, 2017.

38. Pahl HL, Baeuerle PA. (1994) Oxygen and the control of gene expression. *Bioassays* 16: 497–502, 1994.

39. Palande KK, Beekman R, van der Meeren LE, Beverloo HB, Valk PJ, Touw IP. The antioxidant protein peroxiredoxin 4 is epigenetically down regulated in acute promyelocytic leukemia. *PLoS ONE* 6: e16340, 2011.

40. Poillet-Perez L, Despouy G, Delage-Mourroux R, Boyer-Guittaut M. Interplay between ROS and autophagy in cancer cells, from tumor initiation to cancer therapy. *Redox Biol* 4: 184–192, 2015.

41. Prasad S, Gupta SC, Pandey MK, Tyagi AK, Deb L. Oxidative Stress and Cancer: Advances and Challenges. *Oxid Med Cell Longev* 2016: 5010423, 2016.

42. Quan C, Cha EJ, Lee HL, Han KH, Lee KM, Kim WJ. Enhanced expression of peroxiredoxin I and VI correlates with development, recurrence and progression of human bladder cancer. *J Urol* 175: 1512–1516, 2006.

43. Reuter S, Gupta SC, Chaturvedi MM, Aggarwal BB. Oxidative stress, inflammation, and cancer: how are they linked? *Free Radic Biol Med* 49: 1603–1616, 2010.

44. Rolfs F, Huber M, Gruber F, Böhm F, Pfister HJ, Bochkov VN, Tschachler E, Dummer R, Hohl D, Schäfer M, Werner S. Dual role of the antioxidant enzyme peroxiredoxin 6 in skin carcinogenesis. *Cancer Res* 73: 3460–3469, 2013.

45. Scherz-Shouval R, Shvets E, Fass E, Shorer H, Gil L, Elazar Z. Reactive oxygen species are essential for autophagy and specifically regulate the activity of Atg4. *EMBO J* 26: 1749–1760, 2007.

46. Schulte-Hermann R, Timmermann-Trosiener I, Barthel G, Bursch W. DNA synthesis, apoptosis, and phenotypic expression as determinants of growth of altered foci in rat liver during phenobarbital promotion. *Cancer Res* 50: 5127–5135, 1990.

47. Seo MJ, Liu X, Chang M, Park JH. GATA-binding protein 1 is a novel transcription regulator of peroxiredoxin 5 in human breast cancer cells. *Int J Oncol* 40: 655–664, 2012.

48. Soini Y, Kallio JP, Hirvikoski P, Helin H, Kellokumpu-Lehtinen P, Kang SW, Tammela TL, Peltoniemi M, Martikainen PM, Kinnula VL. Oxidative/nitrosative stress and peroxiredoxin 2 are associated with grade and prognosis of human renal carcinoma. *APMIS* 114: 329–337, 2006.

49. Sosa V, Moliné T, Somoza R, Paciucci R, Kondoh H, LLeonart ME. Oxidative stress and cancer: an overview. *Ageing Res Rev* 12: 376–390, 2013.

50. Takano S, Fujibayashi K, Fujioka N, Ueno E, Wakasa M, Kawai Y, Kajinami K. Circulating Glutamate and Taurine Levels Are Associated with the Generation of Reactive Oxygen Species in Paroxysmal Atrial Fibrillation. Dis Markers 2016:

7650976, 2016.

51. Ummanni R, Barreto F, Venz S, Scharf C, Barett C, Mannsperger HA, Brase JC, Kuner R, Schlomm T, Sauter G, Sültmann H, Korf U, Bokemeyer C, Walther R, Brümmendorf TH, Balabanov S. Peroxiredoxins 3 and 4 are overexpressed in prostate cancer tissue and affect the proliferation of prostate cancer cells in vitro. *J Proteome Res* 11: 2452–2466, 2012.

52. Villanueva A, Hernandez-Gea V, Llovet JM. Medical therapies for hepatocellular carcinoma: a critical view of the evidence. *Nat Rev Gastroenterol Hepatol* 10: 34–42, 2013.

53. Wang Z, Li Z, Ye Y, Xie L, Li W. Oxidative Stress and Liver Cancer: Etiology and Therapeutic Targets. *Oxid Med Cell Longev* 2016: 7891574, 2016.

54. Yamada S, Guo X. Peroxiredoxin 4 (PRDX4): Its critical *in vivo* roles in animal models of metabolic syndrome ranging from atherosclerosis to nonalcoholic fatty liver disease. *Pathol Int* 68: 91–101, 2018.

55. Zhang W, Wan X, Liu Z, Xiao L, Huang H, Liu X. The emerging role of oxidative stress in regulating autophagy: applications of cancer therapy. *Cell Mol Biol (Noisy-le-grand)* 63: 67–76, 2017.

56. Zheng N, Liu L, Liu WW, Li F, Hayashi T, Tashiro SI, Onodera S, Ikejima T. Crosstalk of ROS/RNS and autophagy in silibinin-induced apoptosis of MCF-7 human breast cancer cells in vitro. *Acta Pharmacol Sin* 38: 277–289, 2017.

Table 1. Rate of HCC development in WT, *PRDX4*$^{-/y}$ and *hPRDX4*$^{+/+}$ mice 25 weeks after DEN treatment or 24 months under natural condition

	With tumor Number (%)	Tumor-free Number (%)	*P*
Saline-induced			
WT	0(0)	5(100)	
***PRDX4*$^{-/y}$**	0(0)	5(100)	1.0
***hPRDX4*$^{+/+}$**	0(0)	5(100)	1.0
DEN-induced			
WT	3(20)	12(80)	
***PRDX4*$^{-/y}$**	12(80)	3(20)	**0.0028**
***hPRDX4*$^{+/+}$**	1(7)	14(93)	0.598
Natural condition			
WT	0(0)	10(100)	
***PRDX4*$^{-/y}$**	3(43)	4(57)	0.0515
***hPRDX4*$^{+/+}$**	0(0)	10(100)	1.0

Table 2. PRDX4 expression and clinicopathologic factors in patients with HCC

	High expression (n=42) Number (%)	Low expression (n=44) Number (%)	*P*
Age	66.7±1.7	69.0±1.4	0.1536
Gender			0.909
Male	32	35	
Female	10	9	
HBV			0.247
(+)	7	13	
(-)	35	31	
HCV			0.29
(+)	21	16	
(-)	21	28	
Child-Pugh grade			0.615
A	37	36	
B	1	3	
NA	4	5	
Tumor size (mm, mean SD)	32.0±18.5	58.2±43.4	**0.0003**
Number of tumors			0.909
single	32	35	
multiple	10	9	
Tumor differentiation			0.675
Well/moderately	38	37	
Poorly	2	4	
NA	2	3	
Capsular formation			0.704
(+)	34	34	
(-)	8	10	
Capsular invasion			
(+)	29	30	1
(-)	5	4	
Portal vein invasion			**0.046**
(+)	8	17	
(-)	34	27	
Hepatic vein invasion			**0.00952**
(+)	5	17	
(-)	37	27	
Hepatic artery invasion			0.257
(+)	0	3	
(-)	42	41	
Bile duct invasion			0.137
(+)	0	4	

(-)	42	40

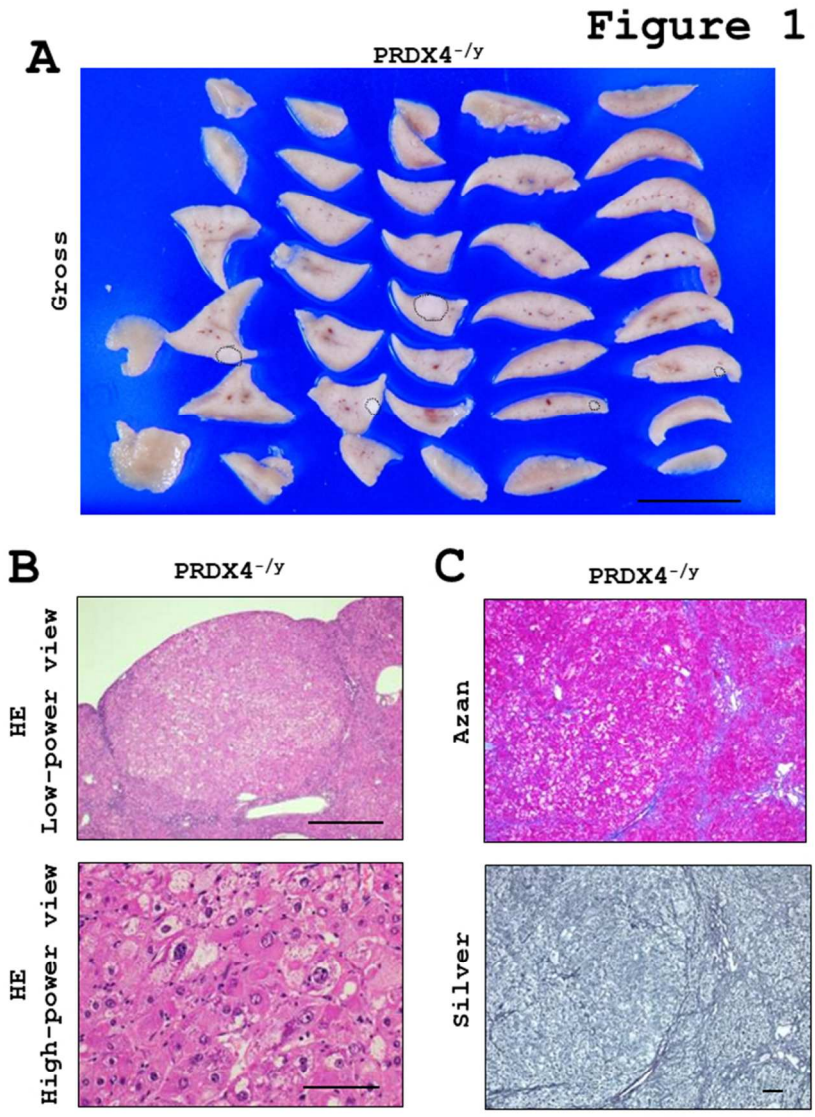

Figure 1

190x254mm (96 x 96 DPI)

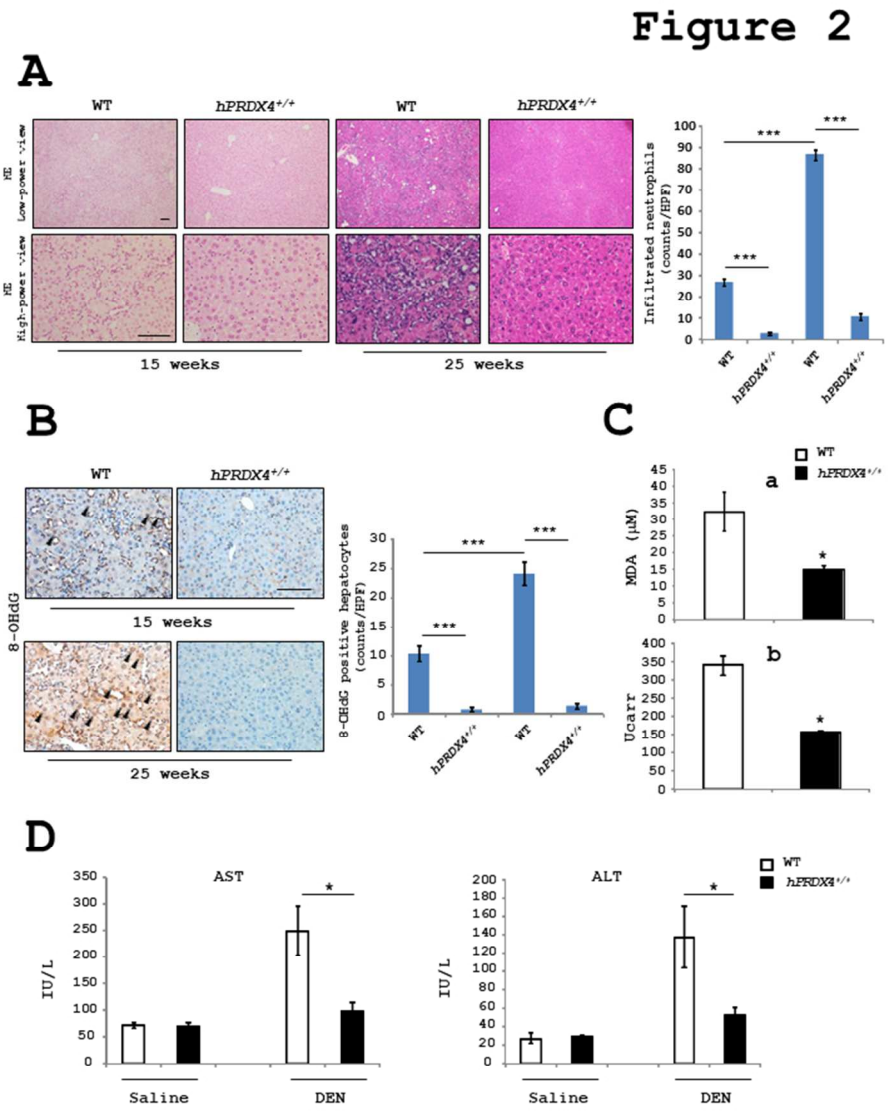

Figure 2

190x254mm (96 x 96 DPI)

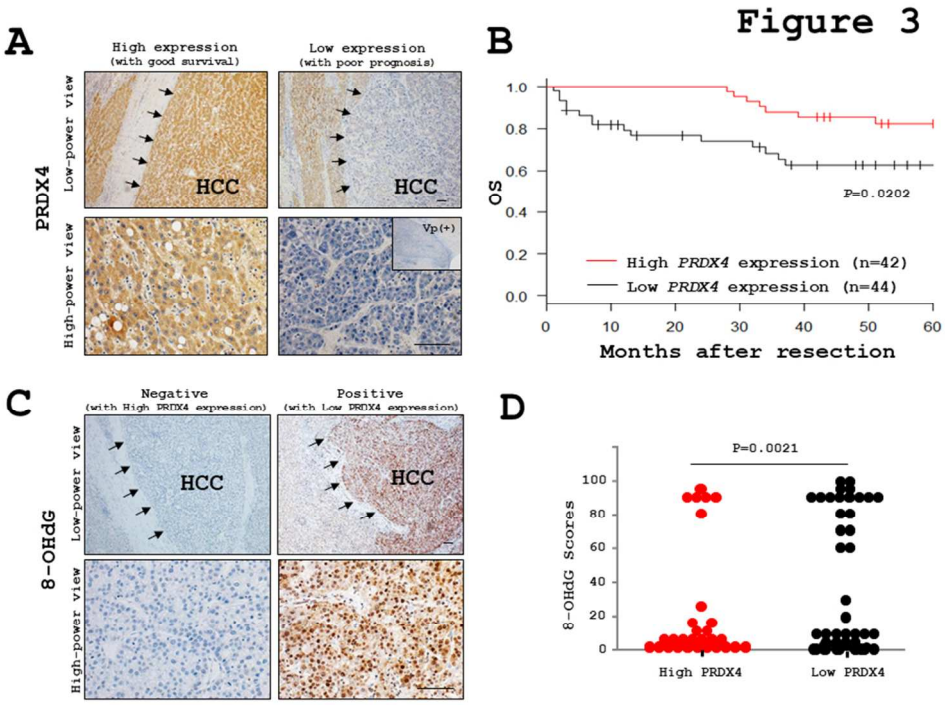

Figure 3

254x190mm (96 x 96 DPI)

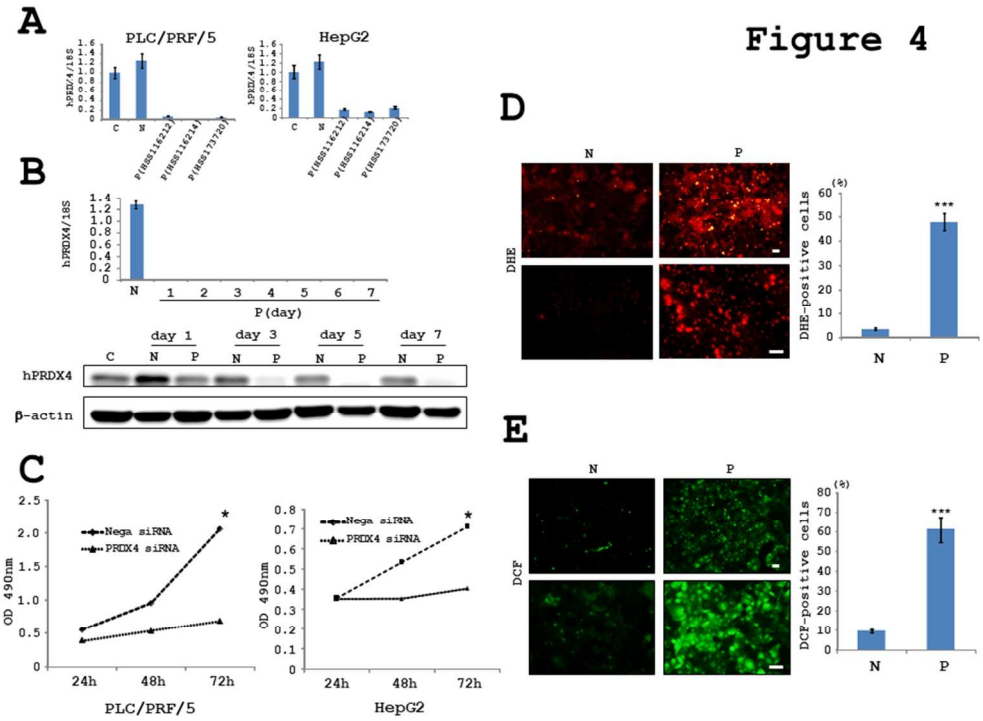

Figure 3

254x190mm (96 x 96 DPI)

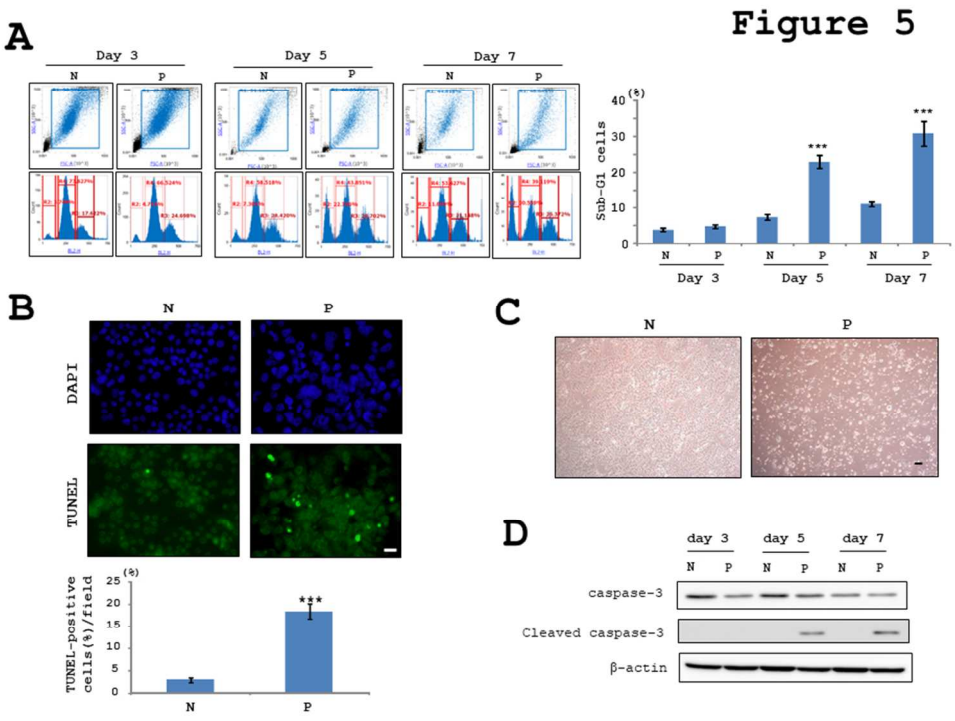

Figure 5

254x190mm (96 x 96 DPI)

Figure 6

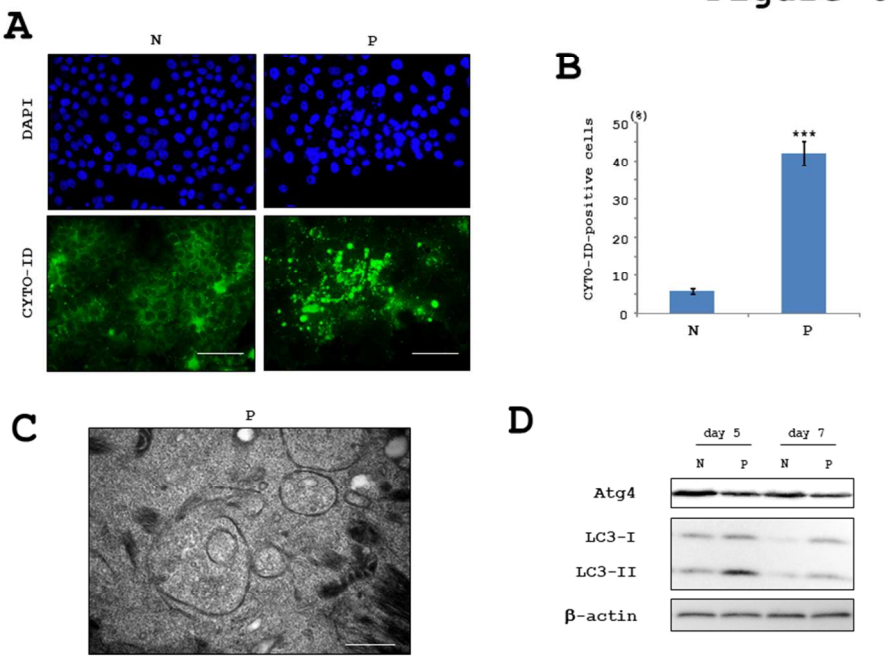

Figure 6

254x190mm (96 x 96 DPI)

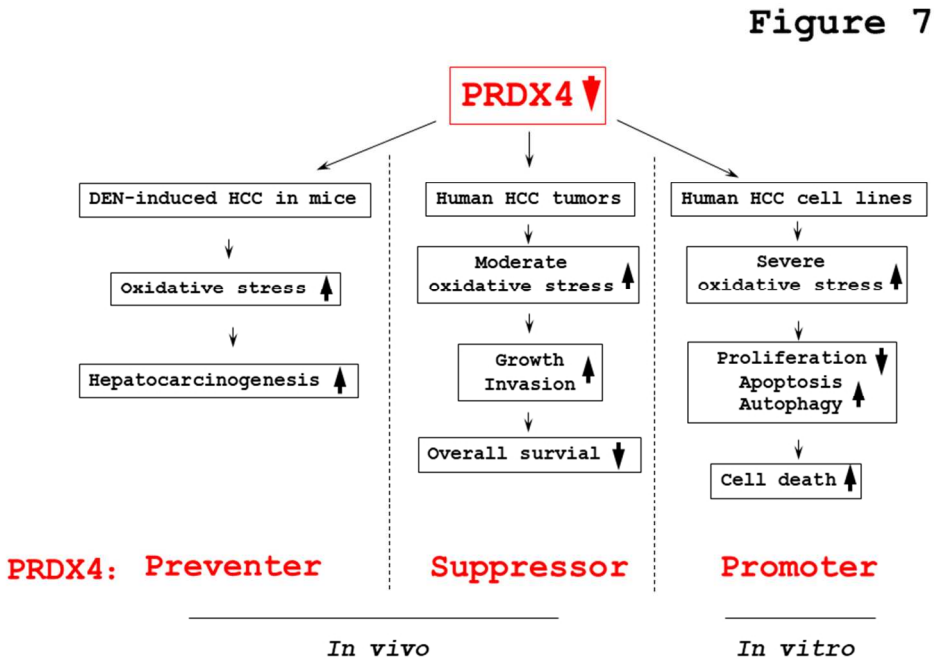

Figure 7

254x190mm (96 x 96 DPI)

Figure legends

Figure 1. DEN induced Multiple HCC tumor in PRDX4$^{-/y}$ mice. (A) The gross picture of the liver in *PRDX4*$^{-/y}$ mice after DEN treatment for 25 weeks, Bar=1 cm. Representative photomicrographs of H&E (B, low-power view, Bar=1 mm; high-power view, Bar=100 μm), azan and silver- (C, Bar=100 μm) stained sections in the liver of *PRDX4*$^{-/y}$ mice after DEN treatment for 25 weeks. n=15.

Figure 2. Overexpression of PRDX4 protected the liver from DEN-induced injury in mice. Representative photomicrographs of H&E- (A) or 8-OHdG- (B) stained sections in the liver of WT or *hPRDX4*$^{+/+}$ mice after DEN treatment for 15 or 25 weeks. Arrowheads, 8-OHdG-positive cells. (C) The MDA level in serum was measured using a TBARS Assay Kit in WT or *hPRDX4*$^{+/+}$ mice after DEN treatment for 25 weeks. (D) The AST and ALT level in serum was measured in WT or *hPRDX4*$^{+/+}$ mice after DEN treatment for 25 weeks. AST, aspartate aminotransferase; ALT, alanine aminotransferase. *P* values were calculated using Welch's *t*-test. The values represent the mean ± SD. Bar=100 μm * P <0.001, ***P < 0.0001, n=15.

Figure 3. High PRDX4 expression reduced the level of ROS in tumor tissues, which is associated with a better overall survival. Representative IHC staining of PRDX4 (A) and 8-OHdG (C) in human HCC tissues. (low-power view 100 x and high-power view 400 x). (B) A Kaplan-Meier's survival analysis of HCC with high

and low PRDX4 expression. (D) Dot distribution graph of 8-OHdG IHC staining scores in high and low PRDX4 HCC tissues. Survival curves were compared using log-rank tests. Categorical variables were compared using the χ^2 test or Fisher's exact test. Bar=100 μm; n=86; $p<0.05$.

Figure 4. Knockdown of PRDX4 inhibited cell proliferation and increased oxidative stress. (A) The PRDX4 expression was examined by real-time PCR in PLC/PRF/5 and HepG2 cells at 72 h after transfection with negative or three kinds of PRDX4 siRNAs. (B) PLC/PRF/5 cells were transfected with PRDX4 (HSS116214) or negative siRNAs in 7 days, and the PRDX4 expression was examined by real-time PCR and Western blotting. (C) Cell proliferation was analyzed using a cck-8 kit 3 days after transfection of siRNAs. ROS production in cells was detected by DHE (D) or DCF (E) staining and fluorescent microscopy. The number of positive cells was counted in 5 random high-power fields. *P* values were calculated using Welch's t test. The values represent the mean ± SD of triplicate experiments. N, negative siRNAs; P, PRDX4 siRNAs; C, non-siRNAs. Bar=100 μm; $p<0.0001$.

Figure 5. Knockdown of PRDX4 induced cell apoptosis. (A) The apoptosis and cycle of cells was analyzed by flow cytometry at 3, 5 and 7 days after transfection with PRDX4 or negative siRNAs. (B) Apoptotic cells were detected by TUNEL staining and fluorescent microscopy 5 days after transfection with siRNAs. The number of positive cells was counted in 5 random high-power fields. (C) The cell

survival status was observed 7 days after transfection with PRDX4 or negative siRNAs. (D) The caspase-3 and cleaved caspase-3 expressions were examined by Western blotting in cells transfected with PRDX4 or negative siRNAs over 7 days. Values were normalized for β-actin expression. *P* values were calculated using Welch's *t*-test. The values represent the mean ± SD of triplicate experiments. N, negative siRNAs; P, PRDX4 siRNAs; C, non-siRNAs. Bar=100 μm; $p<0.0001$.

Figure 6. Knockdown of PRDX4 increased cell autophagy activity. (A) Autophagosomes in cells were detected using the CYTO-ID Autophagy Detection Kit 2.0 at 5 days after transfection with siRNAs, Bar=100 μm. (B) The number of CYTO-ID-positive cells was counted in 5 random high-power fields. (C) The ultrastructure of the cells was observed by electron microscopy, Bar=500 nm. (D) The expression of LC3-I, LC3-II and Atg4 was examined by Western blotting in cells transfected with PRDX4 or negative siRNAs over 7 days. Values were normalized for β-actin expression. *P* values were calculated using Welch's *t*-test. The values represent the mean ± SD of triplicate experiments. N, negative siRNAs; P, PRDX4 siRNAs. $p<0.0001$.

Figure 7. A schematic illustration of the critical roles of PRDX4 in the initiation and progression of HCC.